Cellular and Metabolic Engineering **Biotechnology and Bioengineering**
DOI 10.1002/bit. 21435

Control of Hepatic Differentiation via Cellular Aggregation in an Alginate Microenvironment

Tim Maguire[1], Alexander E. Davidovich[2], Eric J. Wallenstein[1], Eric Novik[1], Nripen Sharma[3], Henrik Pedersen[3], Ioannis P. Androulakis[1,3], Rene Schloss[1], Martin Yarmush[1,3]

1 Department of Biomedical Engineering, Rutgers University, 617 Bowser Road, Piscataway, New Jersey 08854

2 Department of Genetics, Rutgers University, 145 Bevier Road, Piscataway, New Jersey 08854

3 Department of Chemical Engineering, Rutgers University, 98 Brett Road, Piscataway, New Jersey 08854

Corresponding Author:

Martin Yarmush, MD, PhD

Telephone: 732-445-3155

Fax: 732-445-8184

Email: kma@soemail.rutgers.edu

Received October 23, 2006; Accepted March 9, 2007

ABSTRACT

Integral to the development of embryonic stem cell therapeutic strategies for hepatic disorders is the identification and establishment of a controllable hepatic differentiation strategy. In order to address this issue we have established an alginate microencapsulation approach which provides a means to modulate the differentiation process through changes in key encapsulation parameters. We report that a wide array of hepatocyte specific markers is expressed by cells differentiated during a 23 day period within an alginate bead microenvironment. These include urea and albumin secretion, glycogen storage, and cytochrome P450 transcription factor activity. In addition, we demonstrate that cellular aggregation is integral to the control of differentiation within the bead environment and this process is mediated by the E-cadherin protein. The temporal expression of surface E-cadherin and hepatocyte functional expression occur concomitantly and both cellular aggregation and albumin synthesis are blocked in the presence of anti E-cadherin immunoglobulin. Furthermore, by establishing a compartmental model of differentiation, which incorporates this aggregation phenomenon, we can optimize key encapsulation parameters.

KEYWORDS

Alginate, Encapsulation, Hepatocytes, Embryonic Stem Cells, Differentiation

INTRODUCTION

Embryonic stem (ES) cells are characterized by self renewal, pluripotency, and a high proliferative capacity which contributes to a large biomass potential (Gough et al. 1989; Smith et al. 1988). ES cells are therefore a useful cell source for the derivation of renewable adult cell lines, providing the therapeutic potential to assist in the resolution of a variety of devastating illnesses such as heart disease, diabetes, cancer, liver disease, and diseases of the nervous system, such as Parkinson's disease and Alzheimer's disease as well as spinal cord injury (Kiatpongsan et al. 2006; Serakinci and Keith 2006; Taupin 2006; Winkler 2003).

One specific application of ES cells is the derivation of a renewable hepatocyte cell source, needed for the development of bioartificial livers (Balis et al. 2002; Chan et al. 2004; Sharma et al. 2005; Shinoda et al. 2006; Shito et al. 2003; Yarmush et al. 1992), environmental biosensors (Otsuka et al. 2004; Sin et al. 2004), and in vitro drug screening systems (Dambach et al. 2005; LeCluyse 2001). The successful development of these applications lies in expanding a large hepatocyte cell mass. A variety of researchers have designed embryonic stem cell differentiation approaches utilizing growth factor and extracellular matrix protein supplementation to establish a renewable hepatic cell source (Dunn et al. 1989; Kamiya et al. 2006; Novik et al. 2006; Trounson 2006). In an ideal scenario, differentiation of ES cells with these approaches should yield a pure cell population. However, the degree of control during differentiation over the stem cell population using these approaches is limited, especially when bioprocess considerations such as scalability and mass transfer are considered (Dang et al. 2004; Dang et al. 2002; Dang and Zandstra 2004).

We have developed a scalable tissue culture system for the hepatic differentiation of murine embryonic stem cells to address these control issues. We employed a three-dimensional scaffold in the form of alginate encapsulation, which has previously been shown to be a utilitarian construct for precise differentiation of ES cells, as well as a variety of adult stem cells (Maguire et al. 2006; Mehlhorn et al. 2006; Yang et al. 2004). In addition, a wide array of encapsulation parameters may be modified, with potential implications on the hepatic differentiation process. Using this system, and a panel of functional and genomic assays we examined whether we could control the differentiation process. Through changes in two encapsulation parameters, cell seeding density and alginate concentration, which

have been demonstrated to have an effect on cellular function, and in conjunction with a compartmental model, we demonstrated that hepatic differentiation can indeed be modulated using an alginate encapsulation approach.

MATERIALS AND METHODS

Cell Culture

All cell cultures were incubated in a humidified 37°C, 5% CO_2 environment. The ES cell line D3 (ATCC, Manassas, VA) was maintained in an undifferentiated state in T-75 gelatin-coated flasks (Biocoat, BD-Biosciences, Bedford, MA) in Knockout Dulbecco's modified Eagles medium (Gibco, Grand Island, NY) containing 15 % knockout serum (Gibco), 4 mM L-glutamine (Gibco), 100 U/ml penicillin (Gibco), 100 U/ml streptomycin (Gibco), 10 ug/ml gentamicin (Gibco), 1000 U/ml ESGRO™ (Chemicon, Temecula, CA), 0.1mM 2-mercaptoethanol (Sigma-Aldrich, St. Louis, MO). ESGRO™ contains leukemia inhibitory factor (LIF), which prevents embryonic stem cell differentiation. Every 2 days, media was aspirated and replaced with fresh media. Cultures were split and passaged every 6 days, following media aspiration, washing with 6ml of phosphate buffered solution (PBS) (Gibco). Cells were detached following incubation with 3ml of trypsin (Gibco) for three minutes, resulting in a single cell suspension, and subsequently the addition of 12ml of Knockout DMEM. Cells were then replated in gelatin-coated T-75 flasks at a density of 1million cells/ml and only passages 10 through 22 were used in the experiments. In order to induce differentiation, cells were suspended in Iscove's modified Dulbecco's medium (Gibco) containing 20 % fetal bovine serum (Gibco), 4mM L-glutamine (Gibco), 100U/ml penicillin, 100 U/ml streptomycin (Gibco), 10 ug/ml gentamicin (Gibco). The Hepa 1-6 cell line (ATCC, Manassas, VA) was maintained in Dulbecco's modified Eagles medium (Gibco) containing 10% fetal bovine serum (Gibco), 100 U/mL penicillin (Gibco), 100 U/mL streptomycin (Gibco), and 4 mM L-glutamine (Gibco). Hepa1-6 cells were grown on tissue culture treated T-75 flasks (Falcon, BD Biosciences, San Jose, CA), and passages 10 through 22 were utilized for the experiments. Hepa1-6 cells were used as positive controls for each of the following assays.

Alginate Poly-L-Lysine Encapsulation

Alginate encapsulation was carried out as previously described (Maguire et al. 2006). In short, ES cells were encapsulated at an initial cell seeding density of either 1 million, 2 million, 5 million, or 10 million cells/ml in alginate (Sigma-Aldrich, MW: 100,000-200,000 g/mol, G-Content: 65%-70%) poly-L-lysine (PLL) (Sigma-Aldrich,

MW: 68,600 g/mol) (0.05% w/v) beads, at a final alginate concentration of either 1.7%, 2.0%, or 2.5% (w/v). Bead formation was accomplished using an electrostatic bead generator (Nisco, Zurich, Switzerland) which generated beads with an average diameter of 500 um. Polymerization was induced by extrusion of the beads into a 100mM bath of $CaCl_2$ (Sigma Aldrich).

Depolymerization and Cell Recovery

Beads were washed with PBS, and 100mM sodium citrate (Fisher Scientific), containing 10mM MOPS (Sigma-Aldrich) and 27mM NaCl (Sigma-Aldrich) was added for 30 minutes at 37^{o}C to induce depolymerization. The released cells were centrifuged at 1200rpm for 10 minutes, the sodium citrate solution was aspirated, the cell pellet was washed with PBS (3x), and resuspended in cell specific media. The cells were then counted using the trypan blue method.

In Situ Indirect Immunofluorescent Cytokeratin-18 and Intracellular Albumin Analysis

Cells recovered following depolymerization were transferred to a tissue culture treated 24 well plate (Falcon, BD Biosciences). Specifically, the isolated cell population was diluted to $6x10^4$ cells in 0.75 ml of media as was incubated for one hour at 37^{o}C to allow for cell attachment. The cells were then washed for 10 min in cold PBS and fixed in 4% paraformaldehyde (Sigma-Aldrich) in PBS for 15 minutes at room temperature. The cells were washed twice for 10 min in cold PBS and then twice for 10 min in cold saponine/PBS (SAP) membrane permeabilization buffer containing 1% bovine serum albumin (BSA) (Sigma-Aldrich), 0.5% saponine (Sigma-Aldrich) and 0.1% sodium azide (Sigma-Aldrich). To detect intracellular albumin, the cells were subsequently incubated for 30 minutes at 4^{o}C in a SAP solution containing rabbit anti-mouse albumin antibody (150 ug/ml) (MP Biomedicals, Irvine, CA), or normal rabbit serum (150 ug/ml) (MP Biomedicals) as an isotype control, washed twice for 10 min in cold SAP buffer, and then treated for 30 minutes at 4^{o}C with the secondary antibody, FITC-conjugated donkey anti-rabbit, diluted 1:500 (Jackson Immuno Labs, Westgrove, PA). To detect cytokeratin 18, which is produced in mature hepatocytes and a few other mature cell types, cells we incubated for 30 minutes at 4^{o}C in a SAP solution containing rabbit anti-moue cytokeratin 18 antibody (IgG1) (1:50 dilution) (Santa Cruz Biotechnology) or the IgG1 fraction of normal rabbit serum (1:100 dilution) (Santa Cruz Biotechnology) as an isotype control, and then treated for 30 minutes at 4^{o}C with the secondary antibody, FITC-conjugated goat anti-rabbit, diluted 1:200 (Jackson Immuno

Labs, Westgrove, PA). For both stains, cells were then washed once with cold SAP buffer and once with cold PBS. Fluorescent images were acquired using a computer-interfaced inverted Olympus IX70 microscope. Specimens were excited using a 515nm filter. Fluorescent intensity values were determined for each cell using Olympus Microsuite. Experimental intensity values for each cell were calculated after subtracting the average intensity of the isotype control.

Glycogen Staining

Following depolymerization, cells were transferred to tissue culture treated 24 well plates (Falcon, BD Biosciences) and were fixed with 10 % formalin-ethanol fixative solution for 15 minutes at room temperature, with subsequent washes with PBS. Fixed cells were exposed to 0.25 ml of Periodic Acid Solution (Bittner et al.) (Sigma Aldrich) per well for 5 minutes at room temperature. Glycols are oxidized to aldehydes in this process, which is not entirely specific to hepatocytes. After washing cells with PBS to remove the PAS, 1ml of Schiff's reagent was added per well and cells were exposed for 15 minutes at room temperature. Schiff's reagent, a mixture of pararosaniline and sodium metabisulfite, reacts to release a pararosaniline product that stains the glycol-containing cellular elements. A third PBS wash to remove the reagent was followed by image acquisition with an Olympus IX70 microscope and Olympus digital camera.

Sandwich ELISA for Detection of Albumin Secretion

In order to detect secreted albumin within the media supernatants obtained on each of the analysis days, we used a commercially available mouse albumin ELISA kit (Bethyl Laboratories, #E90-134). A standard curve was generated by creating serial dilutions of an albumin standard from 7.8 to 10,000 ng/mL. Absorbance readings were obtained using a Biorad (Hercules, CA) Model 680 plate reader with a 450 nm emission filter. Albumin values were normalized to the cell number recorded on the day of media sample collection.

Urea Secretion

Media samples were collected directly from encapsulated cell cultures on all analysis days. Urea synthesis was assayed using a commercially available kit (StanBio, Boerne, TX). A standard curve was generated by creating serial dilutions of a urea standard from 300 to 0 mg/mL. Absorbance readings were obtained using a Biorad

(Hercules, CA) Model 680 plate reader with a 585 nm emission filter. Urea values were normalized to the cell number recorded on the day of media sample collection.

Statistical Analysis of Functional Assays

Each data point represents the mean of three experiments (each with three biological replicates), and the error bars represent the standard deviation of the mean. We have defined a biological replicate as a tissue culture plate, containing approximately 1500 capsules. Statistical significance was determined using the student t-test for unpaired data. Differences were considered significant when the probability was less then, or equal to, 0.05.

cDNA Microarray Processing and Data Analysis

RNA was prepared from encapsulated cells isolated following depolymerization, in a manner previously reported, (Novik et al. 2006). In general, cells were homogenized, RNA was isolated with a commercially available kit (Quiagen), and RNA was subjected to spectroscopic analysis of quantity and purity, with A260/A280 ratios, at pH 8.0, between 1.9 and 2.1 for all samples. All RNA samples were subsequently subjected to capillary electrophoresis on an Agilent 2100 Bioanalyzer (Palo Alto, CA), with all samples demonstrating sharp 18S and 28S ribosomal RNA bands. Fluorescent probes were then constructed using the Genisphere 3DNA dendrimer system (Genisphere, Hatfield, PA), and hybridized to murine 22k oligo mircroarrays printed at the Rutgers University Keck Center.

The arrays were then scanned on an Axon GenePix 4000B, and intensity values were determined using TIGR Spotfinder (TIGR, Rockville, Maryland). Quality control processing was also conducted with TIGR Spotfinder, and the data was normalized using the Lowess function (Quackenbush 2002) using TIGR Midas (TIGR, Rockville, Maryland). The normalized data set was passed through a series of two filters to obtain a list of annotated genes that demonstrated differential expression in intensity between the experimental and control cases. In filter 1, genes are discarded in each experimental condition if any replicate within either the cy3 or the cy5 data set did not pass the aforementioned TIGR Spotfinder quality control check. The genes that passed this criterion were subjected to a second filter where analysis of variance (ANOVA) was performed to test each gene independently for a statistical difference in expression between the experimental condition and its respective control. In this study we have chosen

to work with ANOVA p value cutoff of 0.05. To calculate the p value, we created an algorithm using the VBA package in Excel (Microsoft, Redmond, WA).

Cloning of the albumin enhancer/promoter and cytochrome p450 7α1 (cyp7a1) promoter driven pDsRedExpress1 vectors

The pDsRedExpress1 plasmid vector was attained from BD Biosciences Clontech (Mountain View, CA). The murine albumin enhancer/promoter was attained in the form of a liver specific expression vector in a pBluescript plasmid from Dr. Joseph Dougherty (UMDNJ-RWJMS, Piscataway, NJ). The cytochrome p450 7α1 (cyp7a1) vector was donated in the form of a PGL3-Promoter vector from Dr. Gregorio Gil (Virginia Commonwealth University, Richmond, VA). The promoter regulatory elements were each excised at a blunt and a sticky end and inserted via ligation into respective blunt and sticky sites in the parent pDsRedExpress1 vector. Correct insertion of the regulatory elements into the pDsRedExpress1 vector was confirmed by screening bacterial clones via test transfections in mouse Hepa 1-6 cells and through DNA sequencing. The two vectors are hereby referred to as pAlb-dsRedExpress1 and pCyp7a1-dsRedExpress1. An additional vector, pDsRed2-C1, driven by the constitutive cytomegalovirus, was used as a control for positive transfection of different cell types.

Transient transfection of liver-specific vectors into stem cells recovered from beads

On day 20, cells were depolymerized and cells were replated on polystyrene plates and allowed to acclimate with the monolayer environment (~72 h). The liver-specific expression vector pCyp7a1-dsRedExpress1, along with the constitutive pDsRed2-C1 plasmid, were transiently transfected into the separate differentiated stem cell populations. A control plate of murine Hepa 1-6 cells was used to assess transient transfection efficiency. Following 24 h, red fluorescent activity was detected via flow cytometry and imaged for fluorescent activity using a computer-interfaced inverted Olympus IX70 microscope. The proportion of cells expressing a liver-specific gene was calculated using the following normalization equation:

$$\%\,\text{cells}(+)\text{for specific gene} = \frac{\left(\frac{\#\,\text{cells}(+)\text{ for liver-specific gene activity in mixed population}}{\#\,\text{cells}(+)\text{ under CMV promoter control in mixed population}}\right)}{\left(\frac{\#\,\text{cells}(+)\text{ for liver-specific gene activity in Hepa1-6 cells}}{\#\,\text{cells}(+)\text{ under CMV promoter control in Hepa1-6 cells}}\right)}$$

Intracapsular Aggregate Size Determination

Beads were sampled from the tissue culture treated T-25 flasks and transferred to 35 mm Mattek dishes (Mattek, Ashland, MA) immediately following encapsulation (day 0), and on the analysis days 8, 11, 14, 17, 20. Bright field images were acquired using a Zeiss Axiovert LSM laser scanning confocal microscope (Germany). Specifically, z-sections of 500 mm diameter beads were taken at 50 mm intervals, to avoid multiple quantification of the same aggregate, for a total depth of 250 mm. Images were quantified using Olympus Microsuite.

In Situ Indirect Immunofluorescent E-selectin and E-cadherin Analysis

To detect E-selectin and E-cadherin, beads were first washed three times with PBS (Gibco) a were subsequently incubated for 30 minutes at 4^{o}C in a PBS solution containing FITC conjugated mouse anti-mouse E-selectin antibody (0.5 ug/ml) (BD Biosciences), FITC conjugated mouse anti-mouse E-cadherin antibody (0.5 ug/ml) (BD Biosciences), or mouse IgG_{2a} (0.5 ug/ml) (BD Biosciences) as an isotype control, and then washed twice for 10 min in cold PBS. Fluorescent images were acquired using a computer-interfaced inverted Olympus IX70 microscope.

Antibody Blocking Experiments

To prevent the formation of aggregates, an E-cadherin or E-selectin antibody was added at a concentration of (0.5 ug/ml) (BD Biosciences) to a 5ml culture sample of beads, in the following step wise manner. In the first experimental case, the antibodies were added for three days of exposure between days 8 and 11 post encapsulation. In the second case, antibody exposure lasted for 6 days, between days 8 and 14. In the third, fourth, and fifth conditions exposure was maintained for 9, 12, and 15 days, respectively, starting at day 8. As a control for non-specific blocking of cell adhesion molecules a mouse IgG_{2a} (0.5 ug/ml) (BD Biosciences) was utilized in a separate 5ml sample of beads. For the control case, the antibody was kept in the presence of the beads for the full duration of the study, 23 days, beginning at day 8 post encapsulation.

Unstructured-Segregated Compartmental Model of Differentiation

To construct the compartmental model of differentiation, we assumed three broad compartments of cells within the differentiation process: 1) undifferentiated cells; 2) differentiated cells; 3) differentiated-aggregated cells. We then

generated mass balances around each of these compartments as follows:

$$\frac{dY_1}{dt} = -k_1 * Y_1$$

$$\frac{dY_2}{dt} = k_1 * Y_1 - k_2 * Y_2$$

$$\frac{dY_3}{dt} = k_2 * Y_2$$

In addition to the cellular mass balances, we also wrote differential equations for the most prominent of our cellular functions, that being albumin secretion.

$$\frac{dY_4}{dt} = k_3 * Y_2 + k_4 * Y_3 + k_5 * \exp(Y_2) + k_6 * \exp(Y_3)$$

Furthermore, the model incorporates the following assumptions and initial conditions:

1. Aggregated cell populations only contain differentiated cells (Figure 5).
2. Cellular death is negligible (Maguire et al. 2006).
3. Differentiated cells do not dedifferentiate in the time period we are studying (Maguire et al. 2006).
4. The effect of cell growth is negated through quantification of the percent of the population which exists in each compartment at each time point, as opposed to the total number in each compartment at each time point.
5. $Y_1(0) = 100 \quad Y_2(0) = 0 \quad Y_3(0) = 0 \quad Y_4(0) = 0$

After formulating the model, we next fit our rate constants to each experimental condition, individually, for the time points between day 0 and day 23 post encapsulation (0, 8, 11, 14, 17, 20, 23). To accomplish this, we utilized the ODE45 solver in Matlab, in conjunction with the fmincon optimizer.

In the next phase of the modeling process, we fit the individual rate parameters to a quadratic equation, again using the fmincon function in Matlab, which incorporates cell seeding density and alginate concentration:

$$\text{Rate Constant} = \alpha_1 * (\text{C}) + \alpha_2 * (\text{A}) + \alpha_3 * (\text{C})^2 + \alpha_4 * (\text{A})^2 + \alpha_5 * (\text{C}) * (\text{A}) + \alpha_6$$

(C) = cell seeding density

(A) = alginate concentration

To run sensitivity analysis on our model, we fit the day 23 model predicted values to another quadratic equation:

$$\text{Normalized Albumin Secretion Rate} = 0.28 * (\text{C}) + 14.62 * (\text{A}) - 0.02 * (\text{C})^2 - 3.59 * (\text{A})^2 - 0.01 * (\text{C}) * (\text{A}) - 14.80$$

(C) = cell seeding density

(A) = alginate concentration

RESULTS

Assessing Hepatic Function within the Encapsulation System

Our previous studies demonstrated the feasibility of differentiating embryonic stem cells within alginate beads. The current studies were initiated in order to determine whether hepatocyte differentiation could be controlled within the alginate microenvironment. Using a previously established set of experimentally optimized encapsulation values (Maguire et al. 2006), (2.0% w/v alginate, $5x10^6$ cells/ml) experiments were designed to assess the expression of a wide array of hepatocyte functional and phenotypic markers during a 23 day differentiation period. As a first measure of lineage commitment, culture supernatant samples were collected and albumin and urea secretion was quantified. The results of these experiments indicate that albumin secretion was initiated at day 11, reached maximum levels at day 20 and plateaued by day 23, **Figure 1A**. In addition, albumin secretion exhibited biphasic kinetic properties, similar to previous studies measuring intracellular albumin production and urea secretion (Maguire et al. 2006). Furthermore, urea secretion, **Figure 1A**, also displays a biphasic peak, though tapers off following the day 20 peak.

To further our analysis of lineage commitment within the bead environment, we examined three other hepatocyte markers, cytokeratin-18 (a hepatocyte cytoskeleton marker), glycogen storage, (used by hepatocytes to store excess glucose), and cytochrome P450 7A1 (Cyp7A1) (a protein necessary for the metabolism of cholesterol within the

liver). Cytokeratin-18 (CK-18) expression during the 23 day culture period was examined following cell recovery from the alginate beads, indirect immunofluorescence, microscopic imaging and image analysis techniques. Specific anti-CK-18 antibody binding was assessed relative to a non-specific immunoglobulin control. As indicated in **Figure 1B**, the CK-18 expressing cell sub-population increased dramatically in the late-stage (day 17-23) of intra-alginate bead differentiation when approximately 70% of the cells were found to be CK-18+. In addition, the temporal expression of Ck-18 was similar to albumin secretion since maximum expression was detected by day 20 and plateaued by day 23.

Glycogen storage, was examined using a colorometric staining procedure, following cell recovery from the alginate beads. Microscopic analysis of stained cells indicated that at the end of the differentiation period, approximately 70% of the population stained positively for glycogen storage, **Figure 1C**. Furthermore, maximal temporal expression at days 20-23, was similar to both albumin secretion and CK-18 expression. In contrast, we were unable to detect stored glycogen in undifferentiated ES cells.

In order to assess Cyp7A1 expression, we used a transfection approach, constructing a GFP tagged Cyp7A1 promoter as a reporter to measure Cyp7A1 transcriptional activity. Transfection with this dynamic gene reporter indicated that the Cyp7A1 promoter was activity measurable by day 20 post encapsulation and suggested that the cells could synthesize the Cyp7A1 protein during the late stage of differentiation (**Figure 1D**). Furthermore, expression at this stage was determined to be (~67% using calculation described in materials and methods) approximately equal to the mature Hepa1-6 control (data not shown).

After determining that Cyp7A1 promoter was activated, we next wanted to determine whether other hepatocyte specific cytochrome P450 (Cyp450) RNAs were also increased. Following depolymerization and cell recovery, cDNA microarray analysis was used to identify Cyp450 mRNAs which were statistically significantly upregulated, within the entire encapsulated population. Gene expression was measured using a 22k complete mouse cDNA microarray and gene expression for the differentiated cells was quantified relative to undifferentiated ES cells. Differential expression was determined with an ANOVA filter of $p<0.05$. These studies indicated that a variety of

Cyp450s (**Table 1**) are differentially expressed and upregulated, including 1A1, 1A2, and 2B9 (Dambach et al. 2005; Hengstler et al. 2005; Yoshinari 2006).

Cellular Aggregation as a Mechanism for Control of Hepatic Differentiation

Our encapsulated cell population analyses suggested a late stage functional increase (day 17-23) that coincided with the onset of cellular aggregation that was previously documented (Maguire et al. 2006). Therefore we hypothesized that the rate and degree of cellular aggregation dictates the resultant degree of hepatic differentiation, with the highest levels of function only being obtainable if the encapsulated cells are in an aggregated state. The role of aggregation in functional regulation of differentiation was initially probed using cDNA microarray analysis to identify upregulated genes known to be important in controlling the process of cellular aggregation (**Table 2**). Next, we used immunofluorescence analysis to examine the cell surface expression of two of these proteins, E-selectin and E-cadherin, within the alginate beads. The results of these experiments indicate that both proteins are upregulated at the later time points of differentiation, and that E-cadherin is expressed at greater levels then E-selectin, **Figure 2A**. Since many studies have previously demonstrated the importance of E-cadherin and E-selectin in the aggregation process, we designed antibody blocking experiments to determine the role of these proteins in cell aggregation and functional differentiation within the alginate beads, as described in the materials and methods section. The results of these experiments indicate that aggregation can indeed be inhibited by blocking the E-cadherin molecule, and that the isotype control does not affect the aggregation process, **Figure 2B**. In addition, the duration of antibody supplementation, was coincident with both the duration of aggregation inhibition as well as recovery of the aggregation response. In contrast, although E-selectin was also expressed on the surfaces of differentiated cells, antibody blocking of E-selectin did not inhibit cell aggregation (data not shown). In addition, both urea and albumin secretion were inhibited following blocking of the E-cadherin, but not E-selectin, protein, **Figure 3**. Furthermore, blocking aggregation and cellular function through the use of E-cadherin antibodies is dependent upon the concentration of antibody added, as indicated in the dose response profiles of cellular aggregation (**Figure 3E**) and albumin secretion (**Figure 3E**), at day 23, following three days of antibody supplementation.

Since these experiments determined that cellular aggregation plays a central role in controlling differentiation, we next wanted to determine whether aggregation could, in fact, serve as the major control point of differentiation

within the bead environment. Therefore, our initial encapsulation parameters were altered as ES cells were encapsulated using 4 different initial cell seeding densities (1 million cells/ ml; 2 million cells/ml; 5 million cells/ml; 10 million cells/ml), and 3 alginate concentrations (1.7%; 2.0%; 2.5%. Experimental analyses indicated that aggregate size could be modulated through changes in alginate concentration (**Figure 4A**) and cell seeding density (**Figure 4B**). Furthermore, by altering the degree of cellular aggregation, the differentiation process, and hence the levels of differentiated function, was also controlled (**Figure 4A, 5B**).

Unstructured-Segregated Compartmental Model of Cellular Differentiation

After determining that the aggregation process is a dominant mechanism underlying differentiation within the bead microenvironment, and that changes in alginate concentration and cell seeding density can be used to modulate differentiation by altering the aggregation process, we wanted to validate that our choice of encapsulation parameters, an initial cell seeding density of 5 million cells/ml and an alginate concentration of 2.0% (w/v), were optimal. In addition, we wanted to know which input parameter the differentiation process is more sensitive. To address these two questions, we chose to use an in silico approach, an unstructured-segmented compartmental model of differentiation, described in the materials and methods section.

As a first step in evaluating the model, we first needed to experimentally validate the assumption that only differentiated cells form aggregates. To do this we utilized an immunohistochemical stain of intracellular albumin for cells maintained within the bead environment. Through this analysis we found that at the later time points in the differentiation process (day 17, 20, 23) only the aggregates stain positive for albumin, **Figure 5**. Thus differentiated cells only exist in the aggregated form at these time points, validating our assumption. Furthermore we also determined that there was not a preference of the antibody to bind to aggregates, since the non-specific binding of the isotype control led to equal intensities both in the single cell form as well as the aggregate form (data not shown).

In the next phase of the modeling process, we used the data from the modulation experiments to fit the rate constants (k_1, k_2, k_3, k_4, k_5, k_6) within the model. For each of the twelve combinations of cell seeding density and alginate concentration, we determined the fraction of cells in each of the compartments, as well as the albumin secretion rate.

We chose to express both metrics as normalized values, since the optimization routine used in the model solution algorithm (see below) is more efficient with these values. To determine the fractions of differentiated and differentiated aggregated cell populations, compared to the undifferentiated cell population, we used immunohistochemical analysis for intracellular albumin production. To distinguish between aggregated and non-aggregated cells, image analysis was first utilized on the bead population to determine the fraction of non-aggregated cells, and then the beads were depolymerized, the aggregates dissociated, and a total cell count was taken. In addition to the population analysis, media samples were taken to analyze secreted albumin content, and were normalized with respect to the albumin secretion rate for hepatocytes (196 ng/million cells/day). Using these data sets, we next fit our rate constants to each experimental condition, individually for the time points between day 0 and day 23 post encapsulation (0, 8, 11, 14, 17, 20, 23). Two representative graphs for the fit of the cell populations can be seen in **Figure 6**. In all of the experimental conditions, we found extremely close fits between experimental and predicted values. In the next phase of the modeling process, we fit the individual rate parameters to a quadratic equation which incorporates cell seeding density and alginate concentration.

With our rate constants determined as a function of alginate concentration and cell seeding density, we next used our model to predict albumin function at day 23, in order to determine the optimum set of input parameters and to see how close our fit is to the experimental values. The maximum level of the normalized albumin secretion rate is predicted to arise with a starting cell seeding density of 5 million cells/ml and an alginate concentration of 2.0% (w/v) which agrees with experimental results, **Figure 7A**. In addition, the normalized albumin secretion rates for these conditions are equal to those values determined experimentally.

The other question we wanted to address was which of the two encapsulation parameters, alginate concentration and cell seeding density, have the most dominant effect on the differentiation process. To do this we fit the day 23 model predicted values to another quadratic equation (materials and methods). The fit of this equation can be seen in **Figure 7B**, and exhibits relatively the same profile as the actual model predicted values, **Figure 7A**. Next we used this fitted equation to run sensitivity analysis. Through our sensitivity analysis we determined two major findings: 1) alginate concentration has a much greater effect on the differentiation process, as seen in the significantly higher coefficient for alginate within the quadratic, as compared to that for cell seeding density. 2) Both alginate

concentration and cell seeding density have a negative effect in higher ranges, as shown by the negative coefficients on the quadratic terms, and as determined experimentally (**Figure 4**).

DISCUSSION

Development of hepatocyte based clinical and pharmaceutical technologies may be improved significantly with the controlled in vitro generation of large numbers of ES-derived cells. In the current studies we evaluated whether modulation of an alginate encapsulated tissue culture environment could be used to control the differentiation of embryonic stem cells, with the end goal of creating a large, renewable hepatic cell source. Our results indicate that using a 23 day alginate bead differentiation strategy, we were able to differentiate cells expressing a wide array of hepatocyte markers. In addition, functional maturity may be dependent upon cellular aggregation within the bead environment, specifically mediated through the E-cadherin protein. In addition, mathematical modeling of the differentiation process demonstrated that cellular differentiation may be controlled through changes in two key encapsulation parameters, specifically, cell seeding density and alginate concentration.

In order to determine the differentiation potential of the alginate encapsulation technique to effectively control the hepatic differentiation of ES cells, we assessed a panel of hepatic functions, using pre-determined optimized encapsulation parameters (Maguire et al. 2006). Through this analysis we found that the differentiated cells obtained through cellular encapsulation were both functionally (**Figure 1**) and genomically (**Table 1, 2**) equivalent to our hepatocyte control, the Hepa1-6 cell line. In addition, the highest levels of functional maturity occurred in the later stages of differentiation, between days 17 and 23 of differentiation. This was true even in the case of albumin secretion (**Figure 1A**) where, although an initial peak occurred between day 8 and 14 post encapsulation, a much larger functional peak was observed at the end of the differentiation period (day 20, day 23). Even more interesting however, is the fact that this temporal progression of function was consistent with our previous studies indicating that cellular aggregation occurred within the bead environment during the later periods of differentiation, after cellular proliferation levels off (around day 8 post encapsulation) (Maguire et al. 2006). We thus developed the hypothesis that the late stage increase in differentiated function was due to cell-cell adhesion of lineage committed cells, with subsequent aggregate formation within the beads. To test this hypothesis we first ran time lapse microscopic analysis and determined that the aggregates arose from cellular aggregation as opposed to mitosis (data

not shown). We also validated that the aggregates were comprised of lineage committed cells, as demonstrated by the following three points. First of all, as shown in Figure 1A, differentiated function, in the form of urea and albumin secretion, is present previous to the onset of aggregation. Second, in generating the data sets to which we fit our subsequent model, we first counted and demonstrated, through immunohistochemical analysis, that the single cells within the capsule do not exhibit differentiated function (Figure 5). We next depolymerized the capsules, dissociated the cellular aggregates, and did a cell count of the total cell population, which upon completing a mass balance, yielded the number of cells in the aggregates. Finally we quantified the number of cells that were positive for intracellular albumin production, and verified that this number was the same as the number of cells contained within the aggregates. Hence the aggregates contain partially differentiated cells. As a third and final point, the greatest increase in aggregate size follows the cellular production and expression of E-cadherin, whose expression is not exhibited by undifferentiated cells. Thus, taken together, one can conclude that the aggregates are comprised of differentiated, albeit not fully differentiated cells, but instead lineage committed cells.

In addition, to validating the key assumptions of our hypothesis, we identified two cell surface proteins, using 22k murine cDNA microarrays, which are integral to cellular aggregation, E-cadherin and E-selectin, and which are also statistically significantly upregulated in our differentiated cell population. It has been reported, in the early stages of differentiation, that E-cadherin production is downregulated (Fok and Zandstra 2005), which agrees with our data from day 0 through day day 8 post encapsulation, as it is not detected in this time period through the use of immunohistochemical analysis, **Figure 2A**. However we do see E-cadherin production later on in the differentiation process, **Figure 2A**. The E-cadherin protein itself has been identified within liver tissue samples, (Figarella-Branger et al. 1995) and has been reported to play a role in hepatic differentiation, (Brieva and Moghe 2004; Dasgupta et al. 2005). Furthermore, the presence of tight junctions facilitated by the presence of E-cadherin, are necessary for normal liver function. When these connections are disrupted, various liver maladies arise, such as in the case of hepatocarcinogenesis, (Gao et al. 2006; Herath et al. 2006; Iso et al. 2005). As a final point, E-cadherin expression has also been documented in other tissue engineering based work, namely the increase in E-cadherin expression of hepatocytes cultured in alginate/galactosylated chitosan/heparin scaffolds (Seo et al. 2006). In addition, E-cadherin presented to mature hepatocytes in the form of modified microspheres, modulated the functional state of the hepatocytes, existing either as a proliferating cell population or a differentially functioning cell population (Brieva

and Moghe 2004). E-selectin too, has been described for modulating cellular aggregation, though it has not been shown to be involved in hepatic differentiation. For example, E-selectin has been shown to mediate macrophage and lymphocyte adhesion to hepatocytes, in a variety of inflammatory response states (Adams et al. 1994; Gong et al. 2006; Kawakami-Kimura et al. 1997; Makondo et al. 2004). Through rigorous antibody based blocking experiments we were able to demonstrate that the E-cadherin molecule is indeed instrumental in our cell aggregation (**Figure 2B**) and differentiation processes (**Figure 3A, 4B**). In these experiments it was determined that while albumin secretion exhibits characteristics similar to the aggregation response i.e. the degree and duration of repression is dependent upon the length of antibody supplementation, urea secretion is altogether blocked, regardless of the duration of antibody supplementation. In addition, albumin secretion does recover to some degree when the antibody is removed from the culture system. Another interesting finding was that although the E-selectin adhesion molecule is expressed on the cell surface, it regulated neither cell aggregation (data not shown), nor differentiated cell function (**Figure 3C, 4D)** in our studies. This may be explained by the fact that, E-selectin has been shown to regulate heterotypic (i.e hepatocyte-leukocyte) as opposed to homotypic cell aggregation (i.e. hepatocyte-hepatocyte) (Edwards et al. 2005).

As a final proof of concept, we evaluated the role of cellular aggregation as a necessary control point to modulate the level of differentiated function. To do this, we used a variety of cell seeding densities as well as alginate concentrations, and we demonstrated that by changing these important encapsulation parameters, we could modulate the resultant size of cellular aggregates as well as the level of differentiated function (**Figure 4**). Through this analysis we also determined that there appears to be an upper limit on aggregate size, since function decreases for the encapsulated cell population at initial cell seeding densities greater then 5 million cells/ml (**Figure 4B**). We hypothesize that this effect may be due to nutrient limitations which could impede the differentiation process, similar to effects seen in other high density culture configurations (Glicklis et al. 2004; Glicklis et al. 2000; Kavalkovich et al. 2002). In addition, it should be noted that cellular aggregation itself is probably not the only controlling factor in cellular differentiation, as growth factors and extracellular matrix proteins have been shown to play a large role in hepatic differentiation (Dunn et al. 1992; Hamazaki et al. 2001; Moghe et al. 1996; Novik et al. 2006). However, we have determined that cellular aggregation is necessary to obtain fully differentiated function, and the actual process of cellular differentiation, upon modulation through key encapsulation parameters, can serve as an important control point in the differentiation process.

Having demonstrated that aggregation is a major regulatory component of the cellular differentiation process, we were next able to construct a mathematical model of differentiation. To do this we used the generally accepted technique of compartmental modeling (Palsson and Bhatia 2004), with special focus on an unstructured segregated model of differentiation (Bailey and Ollis 1986). In an unstructured model, a cell is treated as a whole unit, and hence quantification of processes such as mRNA and protein production is not necessary. A segregated model incorporates the fact that a heterogeneous population exists, such as in the case of cells transitioning from an undifferentiated state to a differentiated state. The advantage of applying this in silico approach is that we are able to ask a variety of questions about the differentiation environment and predict at discrete levels, cellular responses to changes in input conditions, without the full gauntlet of experiments needed to address the same questions. One such question that we sought to answer with the model, was which of the two input parameters had a more pronounced effect on the differentiation process. Through sensitivity analysis of the compartmental model, we determined that alginate concentration had a greater effect on differentiation. Furthermore, from a modeling standpoint, in addition to addressing questions related to the control of differentiation, our compartmental model serves as a basis for future work incorporating scale-up components of the differentiation process, as well as differentiation to a variety of other cell types. Branching out into these areas, however, will require additional transport equations to model scale-up effects, and the determination of new rate parameters for the differentiation of other cell types.

Together, these characterization experiments, modeling approaches, and the results presented herein highlight the importance of identifying key mechanisms of differentiation, such as cellular aggregation, to provide a controllable approach to differentiation. Ultimately cellular encapsulation of ES cells may provide a true solution to the scalable production of a renewable hepatic cell source. To ultimately embrace this technology, however, future work in the areas of scale-up, and in vivo application of the differentiated cells derived with this approach will need to be conducted. In addition, an expanded compartmental model of differentiation, incorporating chemical engineering principals involved in scale-up, will provide a robust view of all key parameters needed to control differentiation at a large scale.

ACKNOWLEDGEMENTS

These studies were supported by NIH DK43371, a grant from the NJ Commission on Higher Education, The Graduate Fellowship Program on Integratively Engineered Biointerfaces at Rutgers (Tim Maguire), the Rutgers-UMDNJ NIH Biotechnology Training Program (Eric Novik and Eric Wallenstein), NSF DGE 0333196, and the Rutgers Undergraduate Aresty Award (Alex Davidovich).

REFERENCES

Adams DH, Burra P, Hubscher SG, Elias E, Newman W. 1994. Endothelial activation and circulating vascular adhesion molecules in alcoholic liver disease. Hepatology 19(3):588-94.

Bailey JE, Ollis DF. 1986. Kinetics of Substrate Utilization, Product Formation, and Biomass Production in Cell Cultures. Biochemical Engineering Fundamentals. New York: McGraw-Hill Book Company. p 373-454.

Balis UJ, Yarmush ML, Toner M. 2002. Bioartificial liver process monitoring and control systems with integrated systems capability. Tissue Eng 8(3):483-98.

Bittner M, Meltzer P, Chen Y, Jiang Y, Seftor E, Hendrix M, Radmacher M, Simon R, Yakhini Z, Ben-Dor A and others. 2000. Molecular classification of cutaneous malignant melanoma by gene expression profiling. Nature 406(6795):536-40.

Brieva TA, Moghe PV. 2004. Engineering the hepatocyte differentiation-proliferation balance by acellular cadherin micropresentation. Tissue Eng 10(3-4):553-64.

Chan C, Berthiaume F, Nath BD, Tilles AW, Toner M, Yarmush ML. 2004. Hepatic tissue engineering for adjunct and temporary liver support: critical technologies. Liver Transpl 10(11):1331-42.

Dambach DM, Andrews BA, Moulin F. 2005. New technologies and screening strategies for hepatotoxicity: use of in vitro models. Toxicol Pathol 33(1):17-26.

Dang SM, Gerecht-Nir S, Chen J, Itskovitz-Eldor J, Zandstra PW. 2004. Controlled, scalable embryonic stem cell differentiation culture. Stem Cells 22(3):275-82.

Dang SM, Kyba M, Perlingeiro R, Daley GQ, Zandstra PW. 2002. Efficiency of embryoid body formation and hematopoietic development from embryonic stem cells in different culture systems. Biotechnol Bioeng 78(4):442-53.

Dang SM, Zandstra PW. 2004. Scalable production of embryonic stem cell-derived cells. Methods Mol Biol 290:353-64.

Dasgupta A, Hughey R, Lancin P, Larue L, Moghe PV. 2005. E-cadherin synergistically induces hepatospecific phenotype and maturation of embryonic stem cells in conjunction with hepatotrophic factors. Biotechnol Bioeng 92(3):257-66.

Dunn JC, Tompkins RG, Yarmush ML. 1992. Hepatocytes in collagen sandwich: evidence for transcriptional and translational regulation. J Cell Biol 116(4):1043-53.

Dunn JC, Yarmush ML, Koebe HG, Tompkins RG. 1989. Hepatocyte function and extracellular matrix geometry: long-term culture in a sandwich configuration. Faseb J 3(2):174-7.

Edwards S, Lalor PF, Nash GB, Rainger GE, Adams DH. 2005. Lymphocyte traffic through sinusoidal endothelial cells is regulated by hepatocytes. Hepatology 41(3):451-9.

Figarella-Branger D, Lepidi H, Poncet C, Gambarelli D, Bianco N, Rougon G, Pellissier JF. 1995. Differential expression of cell adhesion molecules (CAM), neural CAM and epithelial cadherin in ependymomas and choroid plexus tumors. Acta Neuropathol (Berl) 89(3):248-57.

Fok EY, Zandstra PW. 2005. Shear-controlled single-step mouse embryonic stem cell expansion and embryoid body-based differentiation. Stem Cells 23(9):1333-42.

Gao ZH, Tretiakova MS, Liu WH, Gong C, Farris PD, Hart J. 2006. Association of E-cadherin, matrix metalloproteinases, and tissue inhibitors of metalloproteinases with the progression and metastasis of hepatocellular carcinoma. Mod Pathol 19(4):533-40.

Glicklis R, Merchuk JC, Cohen S. 2004. Modeling mass transfer in hepatocyte spheroids via cell viability, spheroid size, and hepatocellular functions. Biotechnol Bioeng 86(6):672-80.

Glicklis R, Shapiro L, Agbaria R, Merchuk JC, Cohen S. 2000. Hepatocyte behavior within three-dimensional porous alginate scaffolds. Biotechnol Bioeng 67(3):344-53.

Gong R, Rifai A, Dworkin LD. 2006. Hepatocyte growth factor suppresses acute renal inflammation by inhibition of endothelial E-selectin. Kidney Int 69(7):1166-74.

Gough NM, Williams RL, Hilton DJ, Pease S, Willson TA, Stahl J, Gearing DP, Nicola NA, Metcalf D. 1989. LIF: a molecule with divergent actions on myeloid leukaemic cells and embryonic stem cells. Reprod Fertil Dev 1(4):281-8.

Hamazaki T, Iiboshi Y, Oka M, Papst PJ, Meacham AM, Zon LI, Terada N. 2001. Hepatic maturation in differentiating embryonic stem cells in vitro. FEBS Lett 497(1):15-9.

Hengstler JG, Brulport M, Schormann W, Bauer A, Hermes M, Nussler AK, Fandrich F, Ruhnke M, Ungefroren H, Griffin L and others. 2005. Generation of human hepatocytes by stem cell technology: definition of the hepatocyte. Expert Opin Drug Metab Toxicol 1(1):61-74.

Herath NI, Leggett BA, MacDonald GA. 2006. Review of genetic and epigenetic alterations in hepatocarcinogenesis. J Gastroenterol Hepatol 21(1 Pt 1):15-21.
Iso Y, Sawada T, Okada T, Kubota K. 2005. Loss of E-cadherin mRNA and gain of osteopontin mRNA are useful markers for detecting early recurrence of HCV-related hepatocellular carcinoma. J Surg Oncol 92(4):304-11.
Kamiya A, Gonzalez FJ, Nakauchi H. 2006. Identification and differentiation of hepatic stem cells during liver development. Front Biosci 11:1302-10.
Kavalkovich KW, Boynton RE, Murphy JM, Barry F. 2002. Chondrogenic differentiation of human mesenchymal stem cells within an alginate layer culture system. In Vitro Cell Dev Biol Anim 38(8):457-66.
Kawakami-Kimura N, Narita T, Ohmori K, Yoneda T, Matsumoto K, Nakamura T, Kannagi R. 1997. Involvement of hepatocyte growth factor in increased integrin expression on HepG2 cells triggered by adhesion to endothelial cells. Br J Cancer 75(1):47-53.
Kiatpongsan S, Tannirandorn Y, Virutamasen P. 2006. Introduction to stem cell medicine. J Med Assoc Thai 89(1):111-7.
LeCluyse EL. 2001. Human hepatocyte culture systems for the in vitro evaluation of cytochrome P450 expression and regulation. Eur J Pharm Sci 13(4):343-68.
Maguire T, Novik E, Schloss R, Yarmush M. 2006. Alginate-PLL microencapsulation: effect on the differentiation of embryonic stem cells into hepatocytes. Biotechnol Bioeng 93(3):581-91.
Makondo K, Kimura K, Kitamura T, Yamaji D, Dong Jung B, Shibata H, Saito M. 2004. Hepatocyte growth factor/scatter factor suppresses TNF-alpha-induced E-selectin expression in human umbilical vein endothelial cells. Biochim Biophys Acta 1644(1):9-15.
Mehlhorn AT, Schmal H, Kaiser S, Lepski G, Finkenzeller G, Stark GB, Sudkamp NP. 2006. Mesenchymal stem cells maintain TGF-beta-mediated chondrogenic phenotype in alginate bead culture. Tissue Eng 12(6):1393-403.
Moghe PV, Berthiaume F, Ezzell RM, Toner M, Tompkins RG, Yarmush ML. 1996. Culture matrix configuration and composition in the maintenance of hepatocyte polarity and function. Biomaterials 17(3):373-85.
Novik EI, Maguire TJ, Orlova K, Schloss RS, Yarmush ML. 2006. Embryoid Body-Mediated Differentiation of Mouse Embryonic Stem Cells Along a Hepatocyte Lineage: Insights from Gene Expression Profiles. Tissue Eng.
Otsuka H, Hirano A, Nagasaki Y, Okano T, Horiike Y, Kataoka K. 2004. Two-dimensional multiarray formation of hepatocyte spheroids on a microfabricated PEG-brush surface. Chembiochem 5(6):850-5.
Palsson BO, Bhatia SN. 2004. Cellular-Fate Processes. Tissue Engineering. Upper Saddle River, NJ: Pearson
Prentice Hall Bioengineering. p 74-81.
Quackenbush J. 2002. Microarray data normalization and transformation. Nat Genet 32 Suppl:496-501.
Seo SJ, Choi YJ, Akaike T, Higuchi A, Cho CS. 2006. Alginate/galactosylated chitosan/heparin scaffold as a new synthetic extracellular matrix for hepatocytes. Tissue Eng 12(1):33-44.
Serakinci N, Keith WN. 2006. Therapeutic potential of adult stem cells. Eur J Cancer 42(9):1243-6.
Sharma NS, Ierapetritou MG, Yarmush ML. 2005. Novel quantitative tools for engineering analysis of hepatocyte cultures in bioartificial liver systems. Biotechnol Bioeng 92(3):321-35.
Shinoda M, Tilles AW, Wakabayashi G, Takayanagi A, Harada H, Obara H, Suganuma K, Berthiaume F, Shimazu M, Shimizu N and others. 2006. Treatment of fulminant hepatic failure in rats using a bioartificial liver device containing porcine hepatocytes producing interleukin-1 receptor antagonist. Tissue Eng 12(5):1313-23.
Shito M, Tilles AW, Tompkins RG, Yarmush ML, Toner M. 2003. Efficacy of an extracorporeal flat-plate bioartificial liver in treating fulminant hepatic failure. J Surg Res 111(1):53-62.
Sin A, Chin KC, Jamil MF, Kostov Y, Rao G, Shuler ML. 2004. The design and fabrication of three-chamber microscale cell culture analog devices with integrated dissolved oxygen sensors. Biotechnol Prog 20(1):338-45.
Smith AG, Heath JK, Donaldson DD, Wong GG, Moreau J, Stahl M, Rogers D. 1988. Inhibition of pluripotential embryonic stem cell differentiation by purified polypeptides. Nature 336(6200):688-90.
Taupin P. 2006. The therapeutic potential of adult neural stem cells. Curr Opin Mol Ther 8(3):225-31.
Trounson A. 2006. The production and directed differentiation of human embryonic stem cells. Endocr Rev 27(2):208-19.
Winkler J. 2003. [Adult neural stem cells: therapeutic potential in neurology]. Med Klin (Munich) 98 Suppl 2:27-31.

Yang IH, Kim SH, Kim YH, Sun HJ, Kim SJ, Lee JW. 2004. Comparison of phenotypic characterization between "alginate bead" and "pellet" culture systems as chondrogenic differentiation models for human mesenchymal stem cells. Yonsei Med J 45(5):891-900.

Yarmush ML, Dunn JC, Tompkins RG. 1992. Assessment of artificial liver support technology. Cell Transplant 1(5):323-41.

Yoshinari K. 2006. [Roles of nuclear receptors in the gene expression of drug-metabolizing enzymes under various physiological conditions]. Yakugaku Zasshi 126(5):343-8.

Table 1: Microarray Data: Hepatic Detoxification Genes

Description	Abbrev.	Expression ratio†	P-value ‡
Cytochrome P450, family 1, subfamily a, polypeptide 1	Cyp1A1	1.343	0.039
Cytochrome P450, family 1, subfamily a, polypeptide 2	Cyp1A2	0.813	0.052
Cytochrome P450, family 1, subfamily b, polypeptide 1	Cyp1B1	2.336	0.000
Cytochrome P450, family 2, subfamily b, polypeptide 9	Cyp2B9	1.786	0.032
Cytochrome P450, family 2, subfamily c, polypeptide 29	Cyp2C29	1.151	0.029
Cytochrome P450, family 2, subfamily d, polypeptide 22	Cyp2D22	1.212	0.003
Cytochrome P450, family 26, subfamily a, polypeptide 1	Cyp26A1	1.478	0.0175
Cytochrome P450, family 3, subfamily a, polypeptide 25	Cyp3A25	1.110	0.0227
Cytochrome P450, family 4, subfamily f, polypeptide 16	Cyp4F16	1.985	0.0403
Cytochrome P450, family 7, subfamily a, polypeptide 1	Cyp7A1	1.201	0.0195

† Expression ratios were calculated as a ratio of the Cy3 intensity value (experimental) to the Cy5 intensity value (control).

‡P-values were calculated using a one-way ANOVA.

Table 2: Microarray Data: Genes Involved in Cell Adhesion Mechanism

Description	Abbrev.	Expression ratio †	P-value ‡
Cytokeratin 18	CK-18	1.20	0.0002
Cadherin 17	CDH17	1.04	0.025
Connexin 26 (Gap junction membrane channel protein beta 2)	GJB2	1.08	0.009
Connexin 32 (Gap junction membrane channel protein beta 1)	GJB1	3.06	0.001
E Cadherin (Cadherin 1)	CDH1	1.93	0.030
E Selectin	SELE	1.50	0.040

† Expression ratios were calculated as a ratio of the Cy3 intensity value (experimental) to the Cy5 intensity value (control).

‡P-values were calculated using a one-way ANOVA.

FIGURE CAPTIONS

Figure 1: Kinetic Profile of (A) Urea and Albumin Secretion, (B) Cytokeratin-18 Expression, (C) Glycogen Staining, and (D) Cytochrome P450 promoter activity. Urea secretion rates were determined using a colorimetric assay, and albumin secretion was determined using a sandwich ELISA. Cytokeratin-18 expression was determined using an immunohistochemical approach. Glycogen staining was determined using a periodic Schiff staining assay. Cytochrome P450 promoter activity was determined through a cellular transfection approach, with a promoter-GFP reporter construct. In all for panels, each data point represents the mean of a sample size of 3 experiments and error bars represent standard deviation of the mean.

Figure 2: Kinetic Profile of E-selectin protein expression and E-cadherin expression on the surface of encapsulated cells (A), and aggregate formation in the presence of E-cadherin antibodies (B). E-selectin and E-cadherin expression was determined with a FITC-conjugated antibody specific for each of the respective cell surface proteins. Aggregate size was determined within the alginate beads using the technique of Z-sectioning using a confocal microscope. Each data point represents the mean of a sample size of 3 experiments and error bars represent standard deviation of the mean.

Figure 3: Kinetic Profile of urea production in the presence of the E-cadherin (A), or E-selectin (C) antibodies, and albumin production in the presence of E-Cadherin (B) or E-selectin (D) antibodies. Urea secretion was determined using a colorimetric assay, and albumin secretion was determined using a sandwich ELISA. In addition, dose response curves were generated for cellular aggregation and albumin secretion following E-cadherin antibody supplementation **(E)**. Aggregate size was determined within the alginate beads using the technique of Z-sectioning using a confocal microscope and albumin secretion was determined through ELISA analysis. Each data point represents the mean of a sample size of 9 samples (3 experiments done in triplicate), and error bars represent standard error of the mean.

Figure 4: Aggregate size and cellular function at day 20 post encapsulation, as a function of alginate concentration (A), and cell seeding density (B). For the alginate concentration studies, ES cells were encapsulated

in 1.7% w/v, 2.0% w/v, 2.5% w/v alginate at a cell seeding density of $5x10^6$ cells/ml, and cultured in Iscove's media. For the cell seeding density studies, ES cells were encapsulated in 2.0% w/v alginate, at cell seeding densities of $1x10^6$ cells/ml, $2x10^6$ cells/ml, $5x10^6$ cells/ml, $1x10^7$ cells/ml, cultured in Iscove's media. Each data point represents the mean of a sample size of nine (3 experiments done in triplicate), and error bars represent standard error of the mean. Asterisks (*) indicate a statistically significant difference from other conditions at day 20.

Figure 5: Intracellular Albumin Intensity as a Function of Aggregate Size Distribution. Albumin intensity values for single cell and cell aggregates were determined using intracapsular immunofluorescence techniques. Each data point represents the mean of a sample size of nine (3 experiments done in triplicate), and error bars represent standard error of the mean.

Figure 6: Experimental and predicted values for population dynamics. (A) 2.0% Alginate and 1 million cells/ml. (B) 2.5% Alginate and 5 million cells/ml. Each experimental data point represents the mean of a sample size of nine (3 experiments done in triplicate), and error bars represent standard error of the mean.

Figure 7: Normalized day 23 albumin secretion values as a function of alginate concentration and cell seeding density. The values used in the plot were either (A) predicted from the model, or (B) generated from the quadratic reduction of the model predicted values.

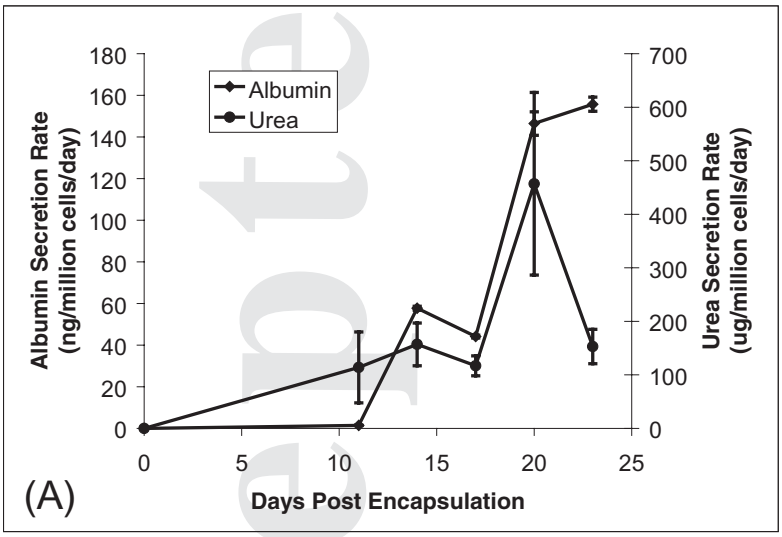
Albumin
Urea
Albumin Secretion Rate (ng/million cells/day)
Urea Secretion Rate (ug/million cells/day)
Days Post Encapsulation
(A)

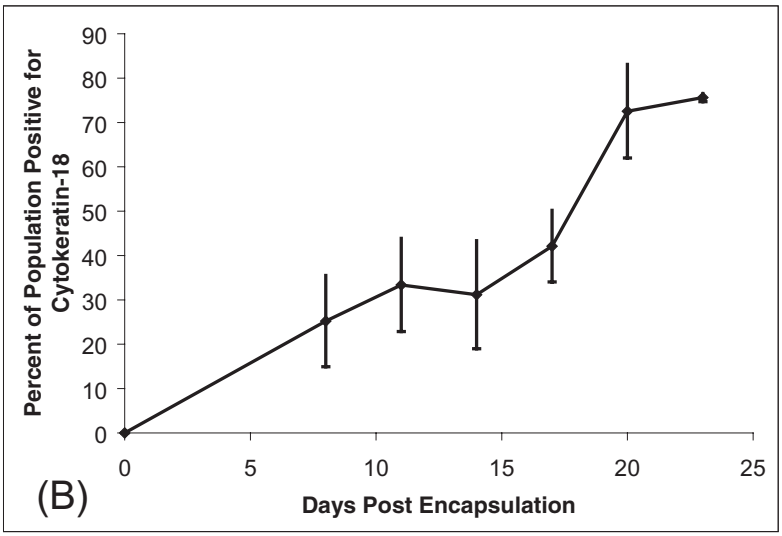
Percent of Population Positive for Cytokeratin-18
Days Post Encapsulation
(B)

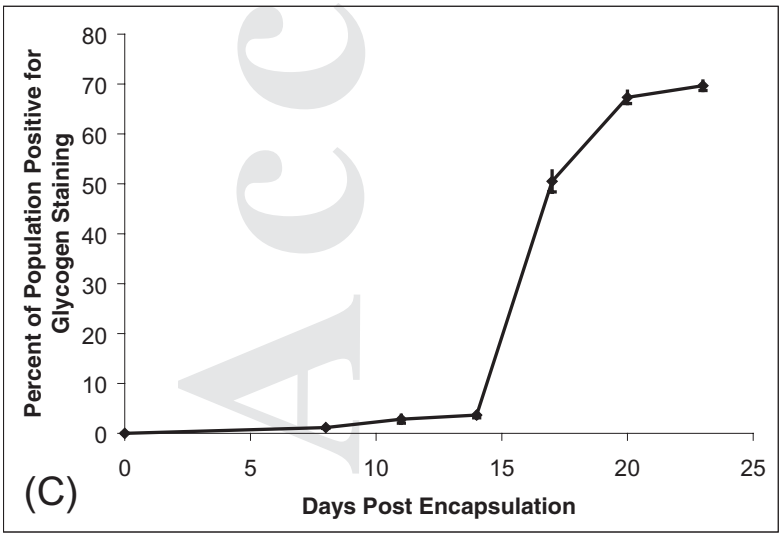
Percent of Population Positive for Glycogen Staining
Days Post Encapsulation
(C)

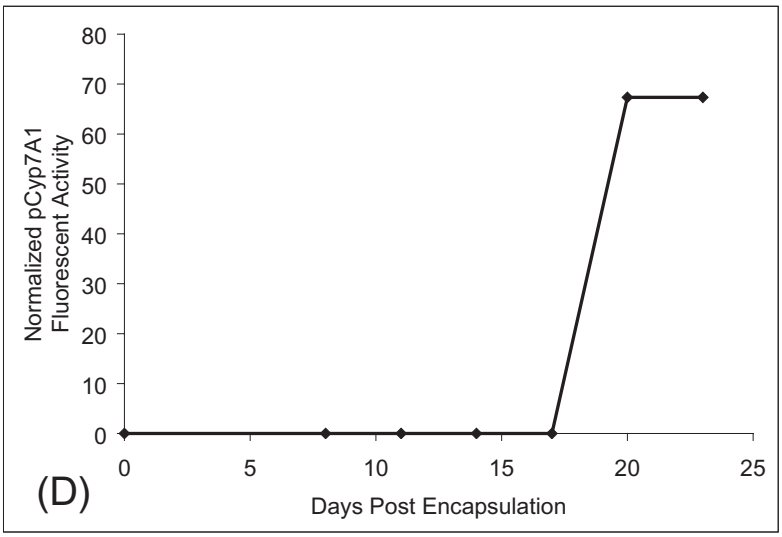
Normalized pCyp7A1 Fluorescent Activity
Days Post Encapsulation
(D)

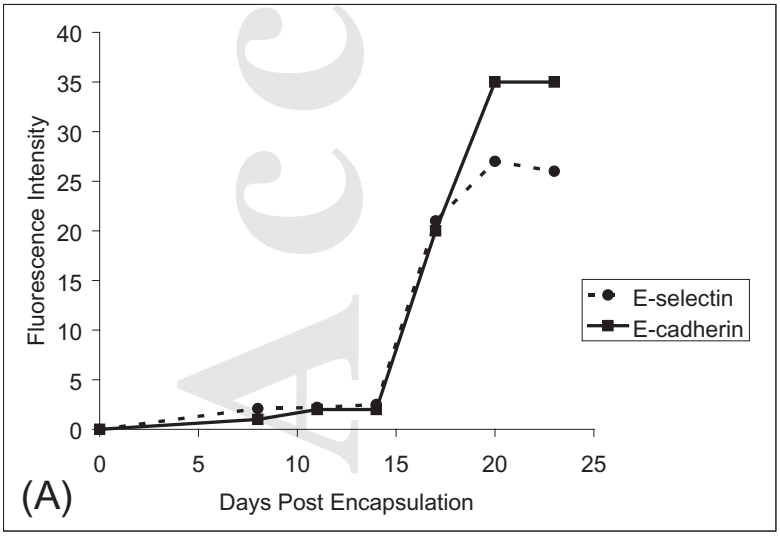
Fluorescence Intensity
40
35
30
25
20
15
10
5
0
0
5
10
15
20
25
Days Post Encapsulation
E-selectin
E-cadherin
(A)

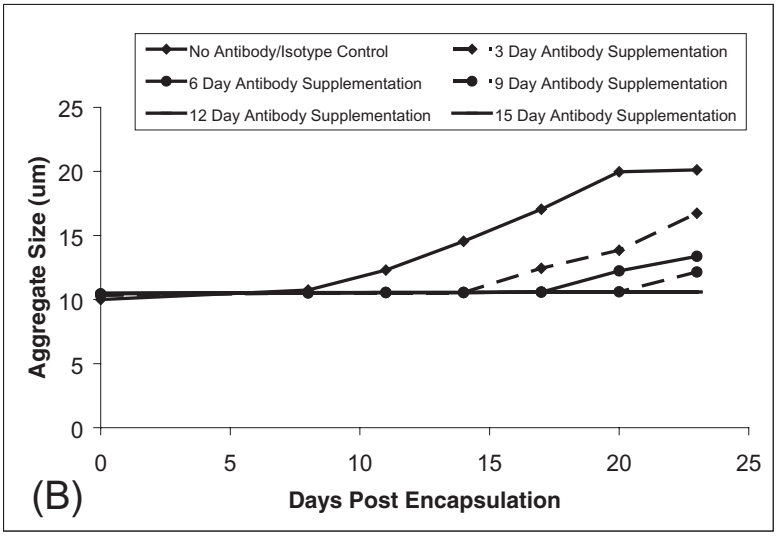
No Antibody/Isotype Control
3 Day Antibody Supplementation
6 Day Antibody Supplementation
9 Day Antibody Supplementation
12 Day Antibody Supplementation
15 Day Antibody Supplementation
Aggregate Size (um)
25
20
15
10
5
0
0
5
10
15
20
25
Days Post Encapsulation
(B)

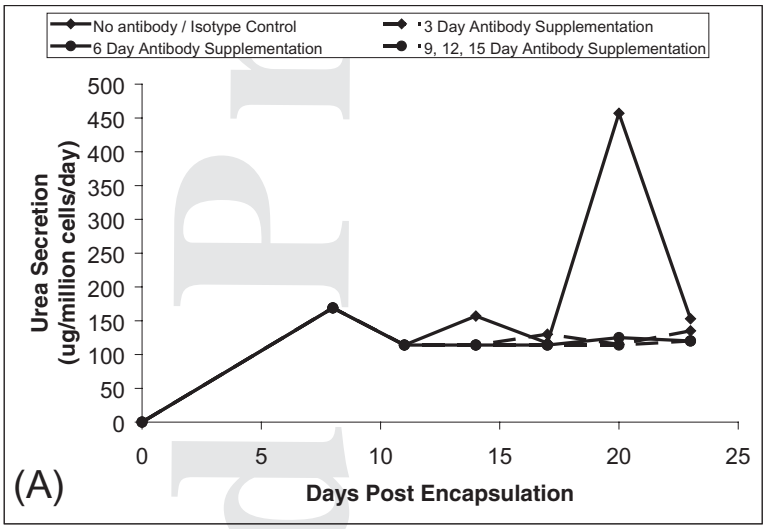
No antibody / Isotype Control
3 Day Antibody Supplementation
6 Day Antibody Supplementation
9, 12, 15 Day Antibody Supplementation
Urea Secretion (ug/million cells/day)
Days Post Encapsulation
(A)

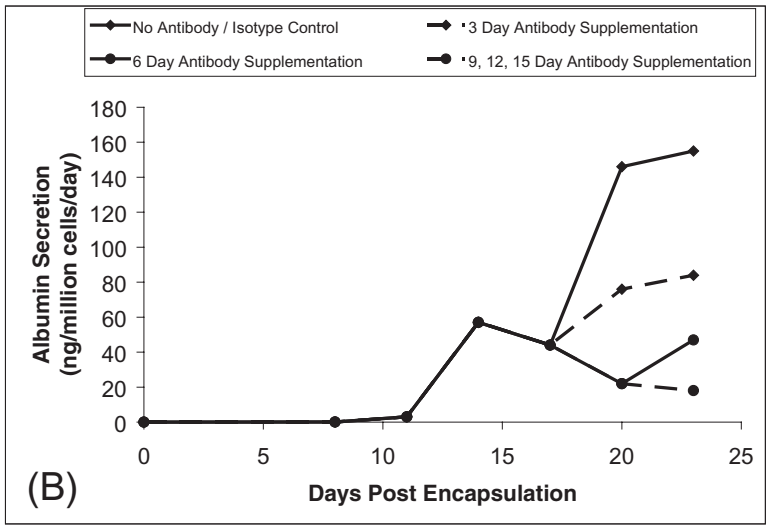
No Antibody / Isotype Control
3 Day Antibody Supplementation
6 Day Antibody Supplementation
9, 12, 15 Day Antibody Supplementation
Albumin Secretion (ng/million cells/day)
Days Post Encapsulation
(B)

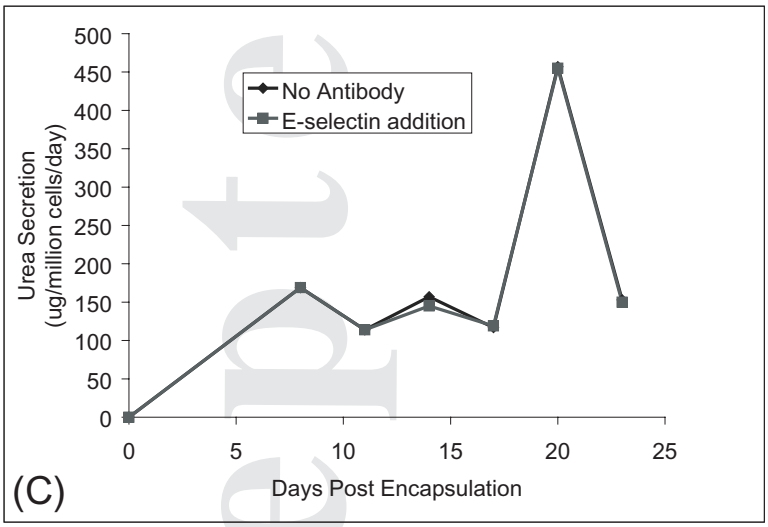
No Antibody
E-selectin addition
Urea Secretion (ug/million cells/day)
Days Post Encapsulation
(C)

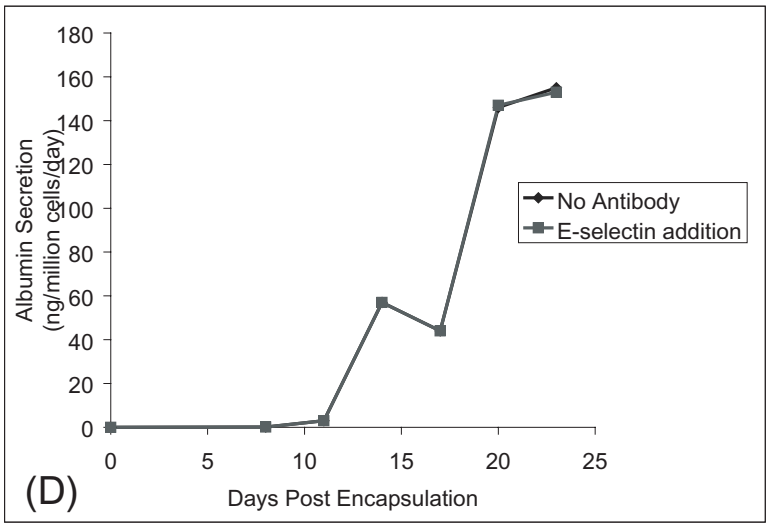
No Antibody
E-selectin addition
Albumin Secretion (ng/million cells/day)
Days Post Encapsulation
(D)

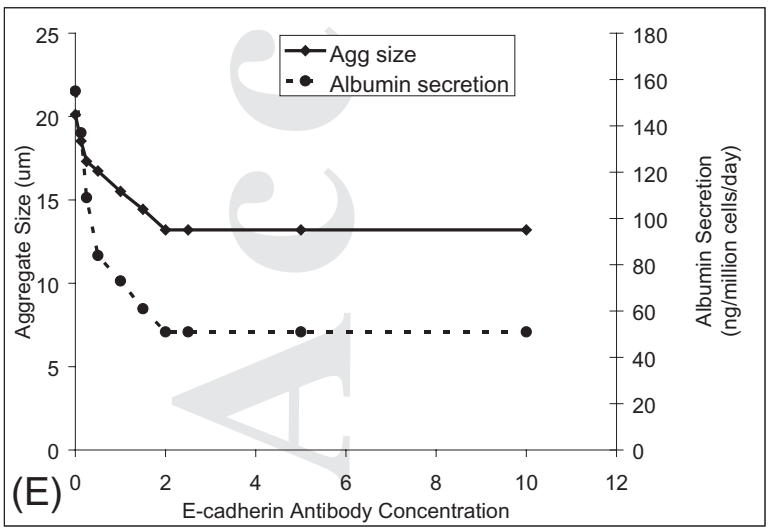
Agg size
Albumin secretion
Aggregate Size (um)
Albumin Secretion (ng/million cells/day)
E-cadherin Antibody Concentration
(E)

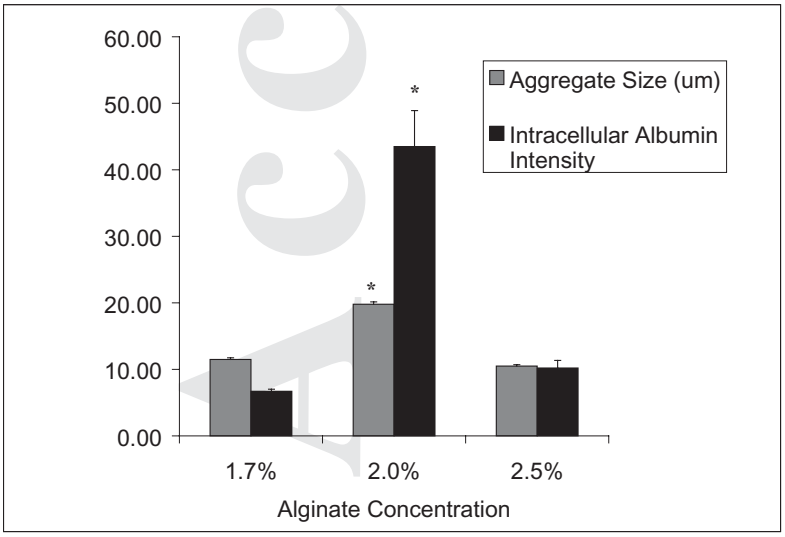
60.00
50.00
40.00
30.00
20.00
10.00
0.00
Aggregate Size (um)
Intracellular Albumin Intensity
*
*
1.7%
2.0%
2.5%
Alginate Concentration

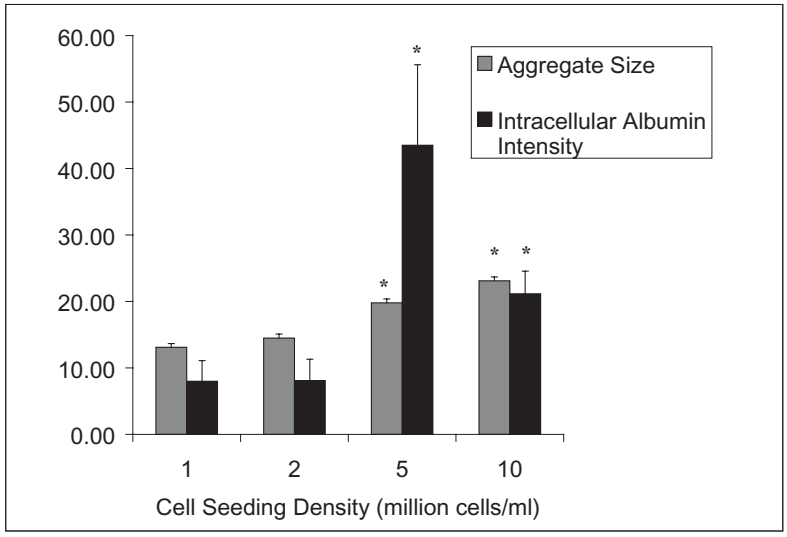
60.00
50.00
40.00
30.00
20.00
10.00
0.00
Aggregate Size
Intracellular Albumin Intensity
*
*
*
*
1
2
5
10
Cell Seeding Density (million cells/ml)

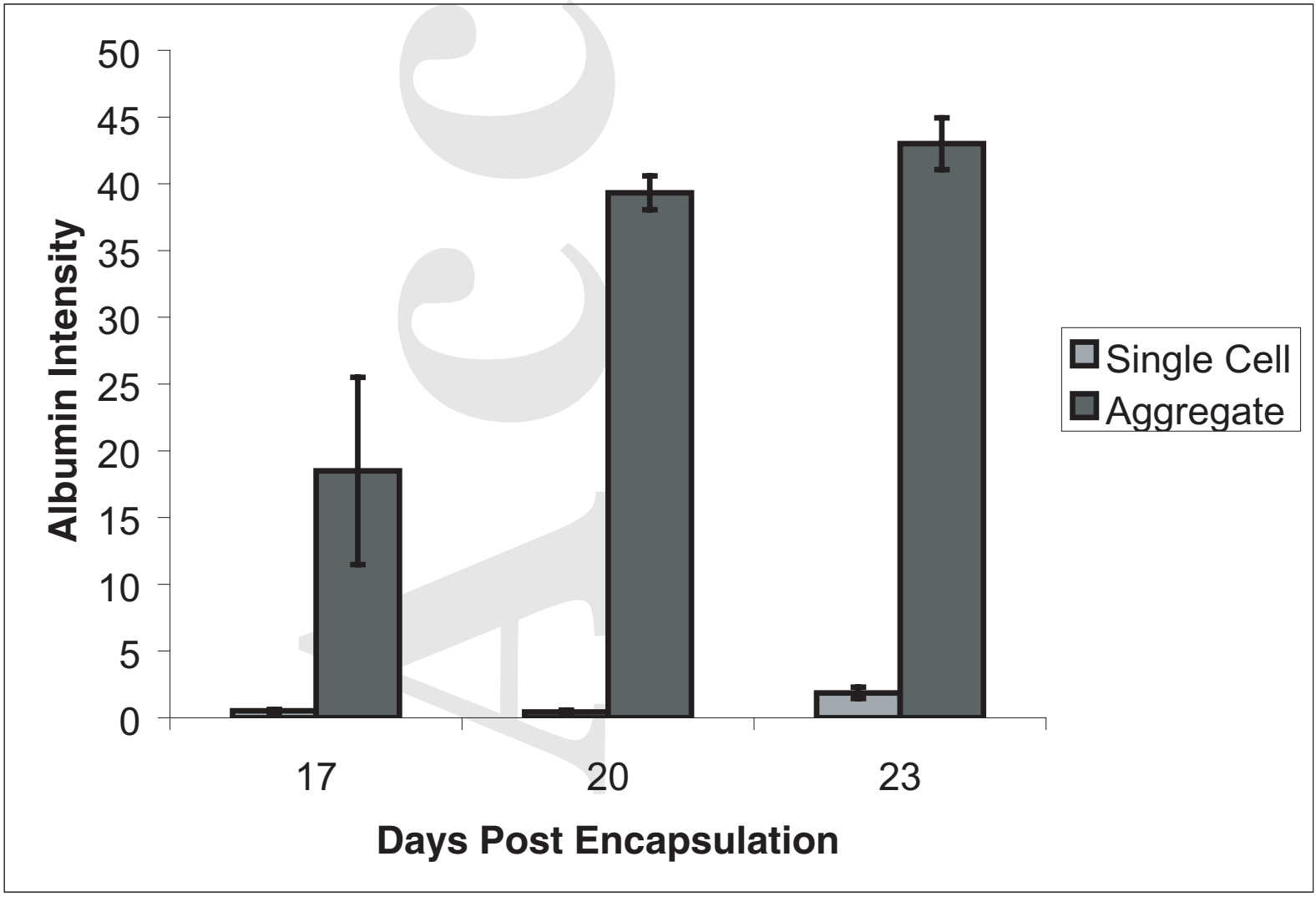
50
45
40
35
30
25
20
15
10
5
0
Albumin Intensity
17
20
23
Days Post Encapsulation
Single Cell
Aggregate

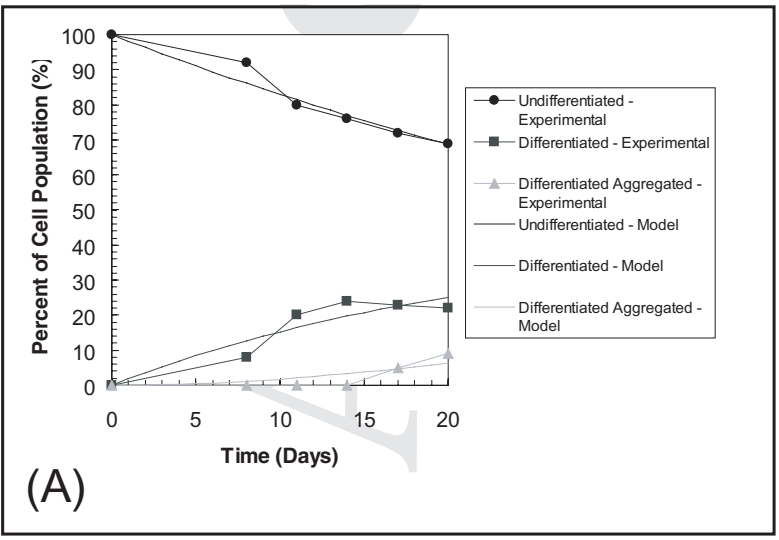
Percent of Cell Population (%)
100
90
80
70
60
50
40
30
20
10
0
0
5
10
15
20
Time (Days)
Undifferentiated - Experimental
Differentiated - Experimental
Differentiated Aggregated - Experimental
Undifferentiated - Model
Differentiated - Model
Differentiated Aggregated - Model
(A)

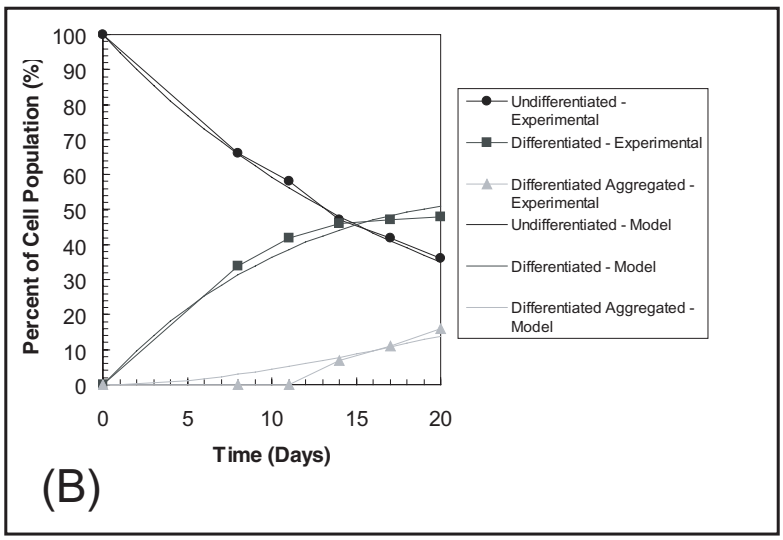
Percent of Cell Population (%)
100
90
80
70
60
50
40
30
20
10
0
0
5
10
15
20
Time (Days)
Undifferentiated - Experimental
Differentiated - Experimental
Differentiated Aggregated - Experimental
Undifferentiated - Model
Differentiated - Model
Differentiated Aggregated - Model
(B)

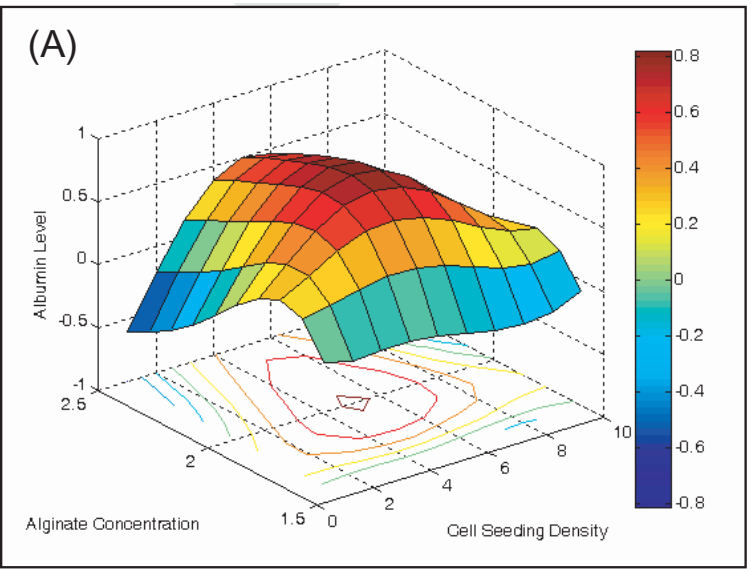
(A)
Albumin Level
1
0.5
0
-0.5
-1
2.5
2
1.5
Alginate Concentration
0
2
4
6
8
10
Cell Seeding Density
0.8
0.6
0.4
0.2
0
-0.2
-0.4
-0.6
-0.8

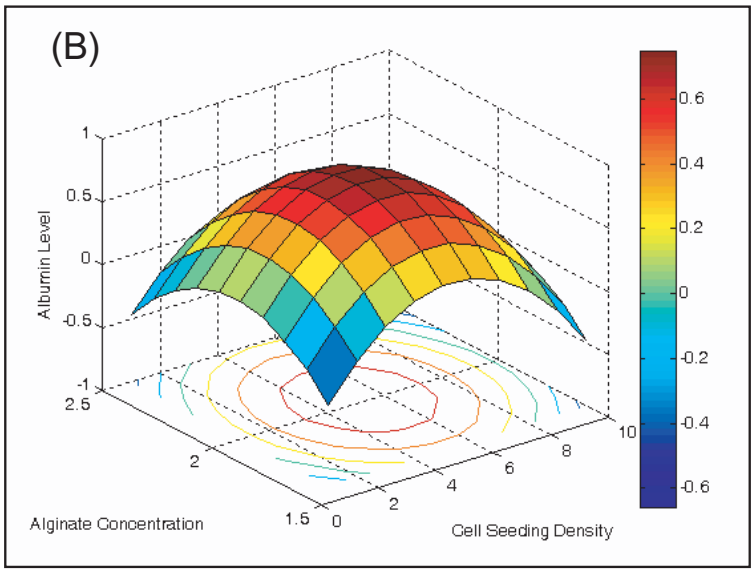
(B)
Albumin Level
1
0.5
0
-0.5
-1
2.5
2
1.5
Alginate Concentration
0
2
4
6
8
10
Cell Seeding Density
0.6
0.4
0.2
0
-0.2
-0.4
-0.6